RSC Advances

This article can be cited before page numbers have been issued, to do this please use: H. Ma, Z. Zhang, Y. Jin, L. Zha, C. Qi, H. Cao, Z. Yang, Z. Yang and Z. Q. Lei, *RSC Adv.*, 2015, DOI: 10.1039/C5RA12154J.

View Article Online
DOI: 10.1039/C5RA12154J

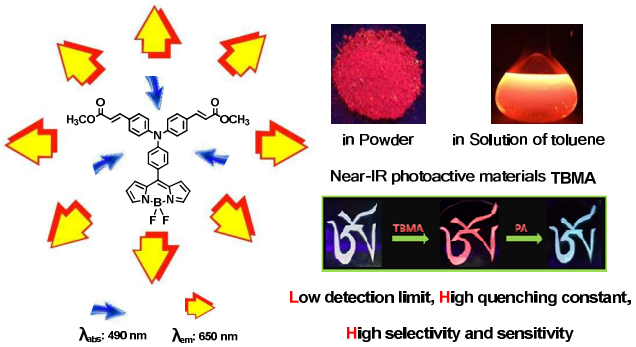

Near-IR photoactive materials TBMA demonstrated high selectivity and sensitivity towards PA detection with low detection limit, high quenching constant.

View Article Online
DOI: 10.1039/C5RA12154J

Triphenylamine-Decorated BODIPY Fluorescent Probe for Trace Detection of Picric Acid

Ma Hengchang,*[a] Zhang Zhongwei, Jin Yuanyuan, Zha Lajia, Qi Chunxuan, Cao Haiying, Yang Zengming, Yang Zhiwang and Ziqiang Lei*[a]

Abstract: Triphenylamine-Decorated BODIPY derivative TBMA was designed and synthesized. Luminogen aggregations were developed through taking advantages of twisted intramolecular charge transfer (TICT) and aggregation-induced emission (AIE) processes. In nonpolar solvents, the locally excited (LE) states of BODIPY luminogens emited intense yellow lights. Increasing solvent polarity brought the luminogens from LE to TICT state, causing a large bathochromic shift in the emission color and a dramatic decrease in emission efficiency. The red emission was greatly boosted by aggregate formation or AIE effect. We also discovered that TBMA could be applied as an efficient chemical sensor for PA detection. The detection limit and quenching constant (K_{SV}) were determined as 30 ppb and $2.1x10^{-6}$ M^{-1} respectively. ^{19}F NMR and ^{1}H NMR titration analysis verified that F···H hydrogen bonding is demonstrated as the interacting mode, which is of possibility to facilitates the effective exciton migration.

Introduction

4,4-Difluoro-4-bora-3a,4a-diaza-s-indacene[1,2] or borondipyrrom-ethene (BODIPY) derivatives are a group of luminogenic molecules that usually emits in the long wavelength region (λ_{em} up to near-IR) in high fluorescence quantum yields (Φ_F up to unity).[3-6] Extensive studies documented that the emission behaviors of BODIPY luminogens are sensitive to the intramolecular rotations and the interactions of their chromophoric segments.[7] However, that is a painstaking work to synthesize BODIPY derivatives with desirable fluorescent property from chemical decorations.[8] Multiple synthetic steps and moderate and low isolated yield always prevent those materials from real applications. It will be really applicable if the intramolecular rotations can be restricted by simple physical processes, if possible, rather than by multi-step chemical modifications. Tang's group has explored the notable aggregation-induced emission (AIE) and aggregation-induced enhancement emission (AIEE).[9,10] As the terms implied that some of luminogenic molecules, for extraordinary instances, triphenylamine (TPA) and tetraphenylethene (TPE) with great freedom in intramolecular rotation are nonemissive when dissolved in their good solvents but become highly luminescent when aggregated in their poor solvents due to the physical restriction on the intramolecular rotations in the aggregates.[11-14] In our previous works, we have been interested in exploring efficient fluorescent materials with intriguing AIE characteristic, and several luminescent molecules have been efficiently prepared and utilized as chemical sensors and smart soft matters.[15,16]

Picric acid (PA) has emerged as a potential explosives due to its high energy release power.[17] In addition, PA is highly water soluble, therefore, which is estimated as major contaminate of groundwater. PA also has been widely used in the dye industry, rocket fuel manufacturing, and the pharmaceutical industry. Thus, for social and living beings' safety, effective monitoring and detection of trace amounts of PA, is really important.[18]

The signal amplification effect, which was discovered for detection of trace amounts of explosives in the solution phase by conjugated polymers, [19-22] has been applied as the traditional

View Article Online
DOI: 10.1039/C5RA12154J

monitoring technology. However, delayed effect is inevitable because of that polymers owing to their very high molecular weight have worse solubility in common organic solvents, leading to reduce their sensitivity and specifity.[23] In recent years, supramolecular polymers employed as chemical sensors turned out to be a potential alternative in this regard. Because of that low-weight molecules can easily be fabricated and modificated diversely, such applicable designing is greatly beneficial to successful exciton migration. Although there were numerous reports on luminescent supramolecular chemosensors for PA detection,[24-26] most detection systems were either less selective or exhibit low-to-moderate Stern-Volmer constants. More than that the ppb level detection in organic solvents was also a crucial but very difficult task. Herein, we report the synthesis and characterization of TPA decorated BODIPY derivative of TBMA (Scheme 1), which was proven to be potential candidates for picric acid sensing with high sensitivity and selectivity.

Results and Discussion

Design and Synthesis of Target Molecules

To enhance the fluorescence response capability of the probes, especially in the visible light region, the target molecule V (abbreviated as TBMA) was designed and synthesized (Scheme 1). There was a triphenylamine (TPA) core with two tentacles like functional group of methyl acrylate (III), which was synthesized from intermediate II by Heck reaction with 85% yield. Importantly, two tentacles are able to induce TPA core be more apparent fluorescent emission due to the formation of conjugated electron donor-accept system. It was also well known that TPA derivatives are of typical AIE prosperities, methyl acrylate groups could provide stronger intermolecular force as we reported.[17] Thanks for the better aggregation ability of the intermediate III, which could emit the desirable green-yellow light under UV light (Scheme 1). Dyes bearing of building blocks of BF_2 complexes of dipyrrin ligands (BODIPYs) have diverse applications as biolabels, artificial light harvesters, sensitizers for solar cells,[27-34] fluorescent sensors,[35,36] molecular photonic wires, and laser dyes.[37,38] This popularity of BODIPY dyes was presumably because of their advantageous spectroscopic properties such as high molar absorption coefficients, narrow band shapes with tunable wavelengths, excitation/emission wavelengths above 500 nm, large Stokes shifts (SS), high fluorescence quantum yields, and considerably high photostability.[39] Therefore, the rigid segment of BODIPY was introduced into TPA core according to Lindsey's procedure by condensing compound III with excess pyrrole in the presence of a catalytic amount of trifluoroacetic acid at room temperature.[40] Afterwards, the dehydration was carried out in dichloromethane with DDQ for 30 min, followed by treatment with triethylamine and $BF_3.OEt_2$ at room temperature for 10 min.[41] Thin-layer chromatographic analysis shown a fluorescent red spot of the desired compound. The crude TBMA were subjected to flash silica gel column chromatographic purification and afforded the stable product V as dark-red solid in 26% yield. Meanwhile, compound VI (abbreviated as TB) was synthesized from intermediate I following the above mentioned method. ^1H, ^{13}C, MS and IR spectroscopies have been used to characterize compounds III, TB and TBMA in detail.

View Article Online
DOI: 10.1039/C5RA12154J

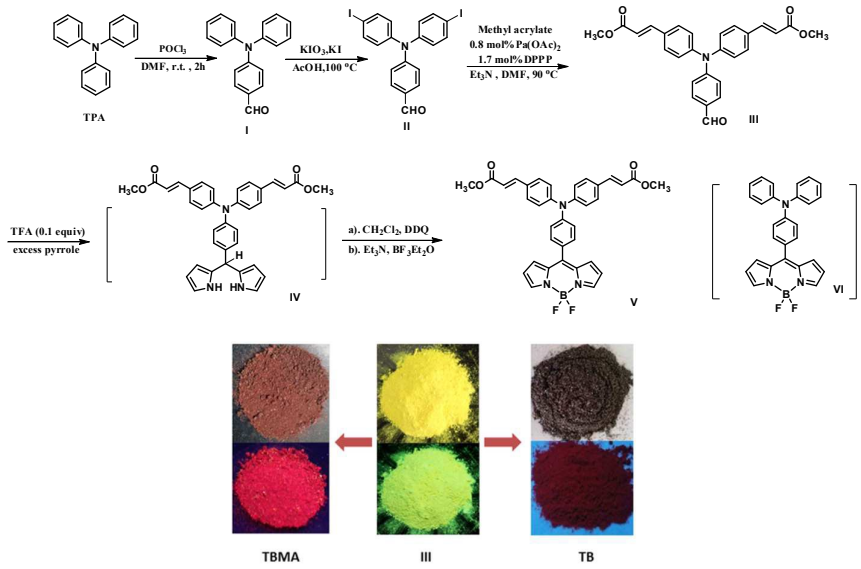

Scheme 1. Synthetic procedures of TBMA(V) and TB(VI), and the photographs of III, TB, TBMA in the powder form under room light (top) and UV light illumination at 365 nm (bottom).

Photophysical properties

Solvent Effect. TBMA shown an almost similar wavelength band, which changes slightly with the variation in solvent as can be seen from the absorption spectra (Fig. 1a). Due to the π-π* transition of the BODIPY unit, a sharp absorption peak (λ_{abs}) appears around at 500-520 nm. As documented that BODIPY derivative with a phenyl ring at the 8 position is much less luminescent (Φ_F = 19%, EtOH), which is due to the rotational movement of the phenyl ring around the single bond nonradiatively deactivates its excited state to a large extent.[42-45] That's to say, the less the rotatable junctions, the higher the emission efficiency. Accordingly, as we synthesized that the bulk junction at 8 position exerts steric effect on the rotational motion of the phenyl ring, such effect was originated from the propeller-shaped TPA core and methyl acrylate groups with strong aggregation ability. Thus, the resulted BODIPY derivative TBMA became more emissive in some cases (as shown in Fig. 1b). The emission study of TBMA in different solvents indicated that the luminescent properties are greatly affected by solvent polarity. The emission band is red-shifted and its intensity is reduced with an increase in the solvent polarity (Fig. S1 and table S1). For instance, fluorescence was almost quenched in the polar solvent of MeOH. However, TBMA shown strong emission and dramatic blue-shift in less polar solvents like toluene (Φ_F = 52%).[46-48]

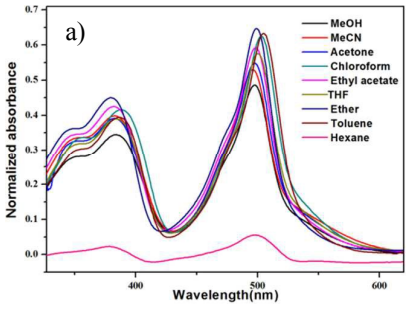

b)

View Article Online
DOI: 10.1039/C5RA12154J

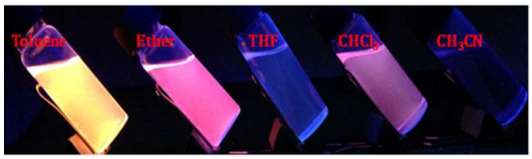

Fig. 1 (a) Normalized absorption spectra of TBMA in different solvents. Solution concentration: 10 μM. (b) Photographs of TBMA in different solvents taken under UV illumination at 365 nm.

TICT Process. To have a deep insight into twisted intramolecular charge transfer (TICT) phenomenon, we serially changed the ratio of solvent by mixing polar THF and nonpolar hexane together. Afterwards, we measured the emission property of TBMA. As can be seen from Fig. 2, When the hexane fraction (f_h) in the THF/hexane mixture was increased from 0 to 90%, the emission color was changed from red to yellow. Meanwhile, the emission was gradually intensified and narrowed into a more sharp band. According to the previous statements that in the locally excited (LE), TBMA may take a more planar conformation. In a nonpolar solvent, the excited luminogen is in equilibrium with solvent molecules and its planar conformation stabilized by a better electronic conjugation gives a sharp emission band. Comparably, in a polar solvent, intramolecular rotation brings the luminogen from LE state to TICT state, in the new equilibrium state, the twisted molecular conformation is stabilized by the polar solvent. Due to the fact that each luminogen molecule has a different twisting angle and hence emission characteristic the collection of which thus gives rise to a broad emission band.[49] This result also could be verified by the temperature-depended emission property in the polar solvent of THF, because the emission of a TICT luminogen was sensitive to temperature variations.[7] From Fig. S2, we could concern that the emission spectrum gently become into a broader band, and the intensity is reduced obviously when the temperature is decreased from 65 to 0 ^{o}C. ^{1}H NMR measurements demonstrated a very different chemical shifts of TBMA in polar and nonpopar deuterium solvents (Fig. 3). As can be seen that in nonpolar toluene-d_8, the crowd peaks in the range of 6.7-7.1 ppm verify the existence of the hydrogen atoms in the C=C double bonds. However, in the solvent of $CDCl_3$, all of them shift to up-field and separate into two cluster of peaks obviously. With increasing the polarity of solvent, (for instance in CD_3CN) two cluster of peaks shift up and down further. Such results clearly confirmed that in the nonpolar solvent of toluene-d_8, a better electronic conjugation renders TPA core with almost equal electron density, thus the nearly equal chemical environments give all of hydrogen atoms in the C=C double bonds with the slight difference of NMR signals. Further, we can concern that TBMA is more prefer to aggregate than mono-dispersein in nonpolar solvent of toluene, because of that all of peaks shifted into up-field apparently. However, in the polar solvent, the D-A electron system formed and a drastic different chemical environments generated two cluster of NMR signals, which further split with the increasing solvent polarity. As we discussed above that TBMA is probable to take more twisted conformation in polar solvent, therefore, a better electronic conjugation is hard to form, which brings about a great different NMR signals. These findings were well agreed with the previous research reports.[7]

View Article Online
DOI: 10.1039/C5RA12154J

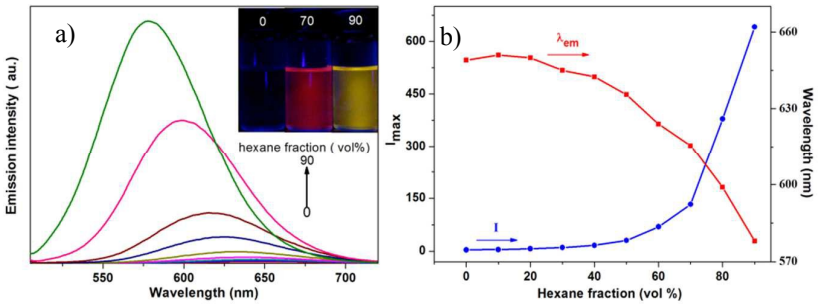

Fig. 2 (a) Emission spectra of TBMA in the THF/hexane mixtures. (b) Plots of maximum emission intensity (I_{max}) and wavelength (λ_{em}) of TBMA versus hexane fraction (f_h) in the THF/hexane mixture. Solution concentration: 10 μM. Excitation wavelength: 490 nm.

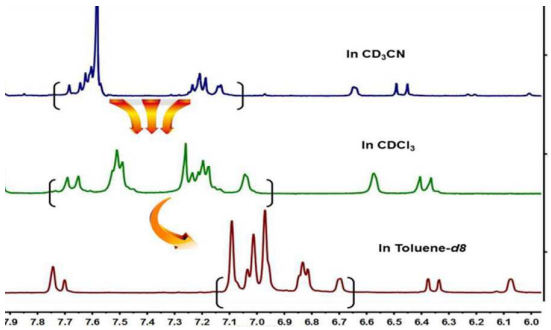

Fig. 3 ^{1}H NMR spectrum (400 MHz, room temperature) of a solution of TBMA in CD_3CN, $CDCl_3$, Toluene-d_8.

AIE Phenomenon. TPA derivatives are typical AIE materials.[50-52] Afterwards, we investigated this physical property in THF/water mixtures according to the documented method. Since TBMA is insoluble in water, they must aggregate in the aqueous mixtures with high water fractions (f_w). And as shown in Fig. 4, the absorption intensity was weaken along with the increasing water fractions, when water fraction was up to 80% in volume, this absorption peak gradually generated two shoulders bathochromicly and hypochromaticly. Those shoulders designated as H- and J-band, are corresponding to the different intermolecular pack modes of H- and J-aggregation.[53,54] From emission spectrum (Fig. 6a), we can see that TBMA is almost non-emissive in pure THF. However, TBMA could emit an intensified red color when 80% water is mixed. To really understand the AIE property and the soft interaction between TBMAs, we carried out ^{1}H NMR titration studies in the mixture of CD_3CN/D_2O (4:1, v/v) and CD_3CN respectively (Fig. 5). Evidently, all of proton resonance signals shifted into up field with different value, which verified the formation of aggregates with increasing D_2O fractions. The changes of chemical shift of the proton resonances of (H_a and H_b) in the double bond displayed the largest Δ value (Δ = 0.04 ppm), and the other identifiable peak of "H_c" demonstrated the smaller Δ value (Δ = 0.02 ppm), such results indicate the detectable interactions may take place between the interlaced tentacles like functional group of methyl acrylate. More than that the obvious H-H NOESY correlations of TBMA could be detected as shown in Fig. 6b, such correlations are originated from an attractive interaction between superimposed phenyl and carbonyl groups of methyl ester. Therefore, what could be confirmed that in the mixture of CH_3CN/H_2O=1:4, the well-organized aggregates are formed in H- and J-pack modes by C=O...π interactions, which results in AIE phenomenon. All the mixed solutions were macroscopically homogeneous and transparent with visible tyndall effect,

View Article Online
DOI: 10.1039/C5RA12154J

suggesting that the aggregates are nanosized. The formation of nanoaggregates was supported by SEM images that when f_w= 20%, uniformed nano-spheres scattered on the silicon wafer, where as long as several micrometer's fibres enlaced each other in the case of f_w= 80% (Fig. 6c). Accordingly, reversible macro-gels could be easily formed. In tremendous comparison, if TBMA doesn't possess two tentacles like methyl acrylate groups (for instance of compound TB), no fibres could emerge, let alone gel formation (Fig. S6). The details of gelation ability could be seen in Supporting Information.

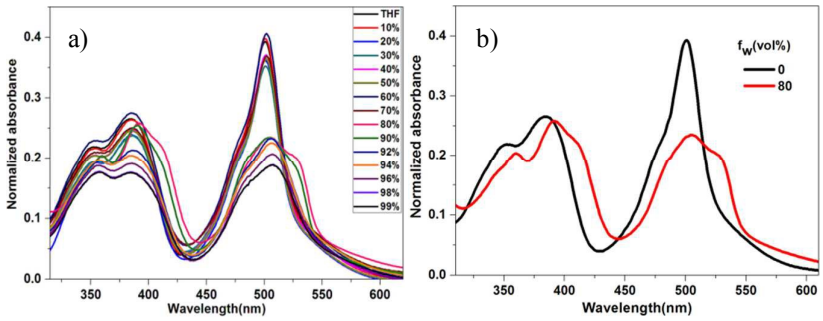

Fig. 4 (a) Normalized absorption spectra of TBMA in THF/water mixtures. Solution concentration: 10 μM. (b) Normalized absorption spectra of TBMA(10 μM) in f_w= 0 and 80%.

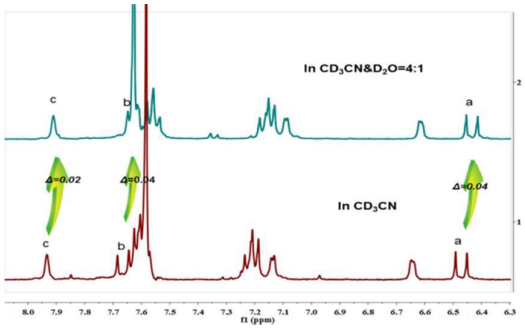

Fig. 5 ^{1}H NMR spectrum (400 MHz, room temperature) of a solution of TBMA in CD_3CN, and CD_3CN/D_2O(v/v = 4:1).

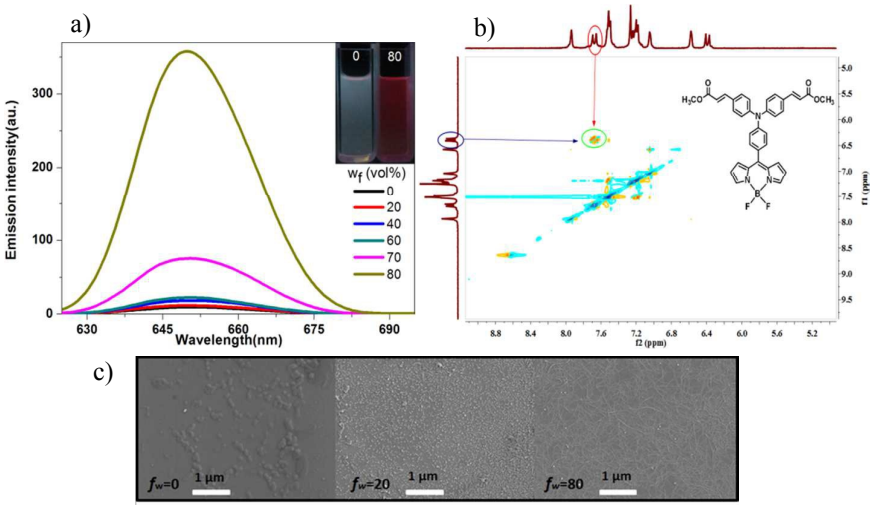

Fig. 6 (a) Emission spectra of TBMA in the THF/water mixtures. Solution concentration: 10 μM.

View Article Online
DOI: 10.1039/C5RA12154J

Excitation wavelength: 500 nm. (b) The NOESY NMR spectrum (400 MHz, room temperature) of a solution of TBMA in $CDCl_3$. (c) SEM image of TBMA in the different the water fraction (f_w).

In order to verify the interactions between TBMA and solvent, we prepared the gel of TBMA in $CH_3CN\&CH_3CH_2OH$, then casted it on the quartz plate. The real-time FT-IR spectra were recorded during solvent vaporization, which clearly displayed that two identical absorption bands around 1710 cm^{-1} are narrowed into one sharp peak after less than 30 min, which was recognized as C=O absorption peak. This transformation confirmed the hydrogen bonding formation between C=O of TBMA and CH_3CH_2OH. Additionally, in contrast with powders of TBMA, the xerogel of TBMA demonstrated more sharp resonance peaks in IR spectrum (Fig. S7), this difference possibly implied that in the xerogel state (Fig. S8), TBMAs are well-organized than in the powder state, therefore, more uniformed aggregation modes bring about the narrow distributed resonance energy of C=O.

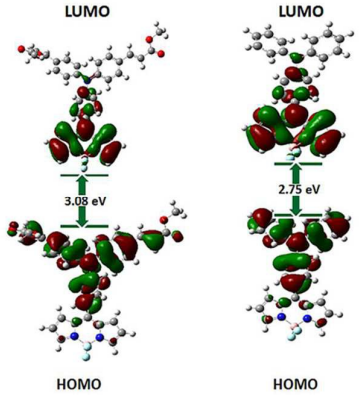

Fig. 7 The optimized molecular orbital amplitude plots of HOMO and LUMO energy levels of TBMA (left), TB (right).

We performed density functional theory (DFT) calculations to gain a better understanding of the geometric and electronic structure and optical properties of the molecules presented in this study. Thus, quantum chemical optimization on their energy levels based on DFT/B3LYP/6-31G (d,p) using Gaussian 09 is conducted. Fig. 11 displayed the highest occupied molecular orbital (HOMO) and lowest unoccupied molecular orbital (LUMO) diagrams of TBMA and TB. According to Fig. 7, both HOMO of these compounds were basically distributed over the TPA cores, and LUMO of TBMA and TB extended across the BODIPY frames, which indicated that these derivatives have obvious ICT tendency.[55] This result was also consistent with the observed stronger solvent dependence fluorescence behaviours of TBMA and TB. Compared with TB, TBMA has a lower higher energy (−5.58 eV), which is due to the existence of electron with drawing methyl acrylate groups, and a lower LUMO energy (−2.85 eV), because of that the less distorted structure is favorable for decreasing the LUMO energy.

Detection of Nitroaromatic Explosives in Solution

Quenching Studies

In the sensing behaviors of PA toward TBMA, the fluorescence titration for sensor with PA revealed that fluorescence emission intensity are rapidly died down upon addition of increasing amounts of PA solution (Fig. 8, S9), the quenching efficiency was found to be 95%. Obviously, SEM images (Fig. 8b) demonstrated that long fibres are disrupted into cluttered sticks in the

View Article Online
DOI: 10.1039/C5RA12154J

presence of PA. These results demonstrated the interactions of TBMA with PA possibly occurs.

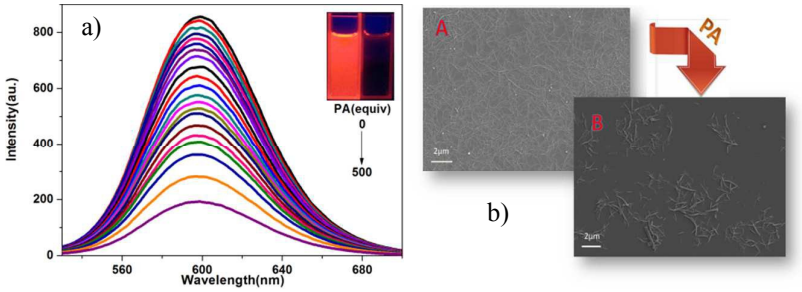

Fig. 8 (a) Fluorescence spectrum of TBMA on addition of PA(0-500eq.) in toluene respectively. Insets show the quenching in fluorescence of TBMA after addition of PA. Solution concentration: 10 μM. Excitation wavelength: 500 nm. All images are taken under 365 nm UV lamp. (b) SEM images of TBMA (A) and TBMA&PA (B).

To check the portable application of the sensor in more convenient manner, we prepared the easily available filter paper as the substrate material. For more visualized exhibitions (Fig. 9), filter paper is cut into a Tibetan language word, then, which was moistened by TBMA solution (10^{-4} M in toluene). After evaporating the solvents, the test paper is immersed into the solution of PA (10^{-4} M in toluene). Obviously, the luminescent decay happened once dipping the test paper into the solution of PA. These results clearly displayed the practical applicability of TBMA for the instant visualization of traces of PA.

Fig. 9 Paper strips of compound TBMA (10^{-4} M) for PA (10^{-4} M) detection.

Quenching Mechanism

We explored the interaction models of TBMA with PA investigated by ^{19}F NMR spectroscopic analysis carried out in $CDCl_3$ (Fig. 10). As several recently reported BODIPY compounds that the fluorines are found to be inequvalent and show two sets of multiplets at -140 ppm.[41,56] However, in the mixture of TBMA with PA, we observed only one quartet in ^{19}F NMR, indicating that the fluorines are under a chemically equivalent environment. Notably, in the presence of PA, the ^{19}F NMR signal of TBMA exhibits obvious downfield shift. This unusual downfield shift was probably attributed to the presence of hydrogen bonding between fluoride ions and PA. Such observation was also consistent with the reported dipyrromethene dyes.[57] Meanwhile, TBMA was possibly disfavor the formation of aggregates in the presence of PA due to the huge steric hindrance after producing complex VII. Thus, the AIE process was suppressed, and leading to the disappearance of emission color. Additionally, the significant emissive performances represent two different "states", where the fluorescence is "switched on" (state I) without PA and "switched off" (state II) with PA, as shown in Scheme 2. In the presence of PA, the intermolecular photoinduced electron transfer (PET) could be potentially enhanced after capturing the more acidic molecules of PA, because BODIPY core turns into a more electron-deficient center. The another way, PA or picrate (P^-) ions promotes the PET quenching of the TPA excited state effectively. Furthermore, the intermolecular bonding models were

View Article Online
DOI: 10.1039/C5RA12154J

verified by ^{1}H NMR titration analysis. From Fig. 11, we can see that the signals of hydrogen atom in -OH group of PA up-field shifted and become broaden gradually with increasing the concentration of sensor of TBMA. Comparably, all of rest peaks displayed negligible chemical shift. Therefore, these results confirmed the formation of complex VII by definite interacting patterns of F···H hydrogen bonding. What's more, this conclusion also inspired us that dipyrromethene dyes possibly could be applied as specific chemical sensors to phenol derivatives. Especially, more acidic the analytes, more sensitive the BODIPY sensors.

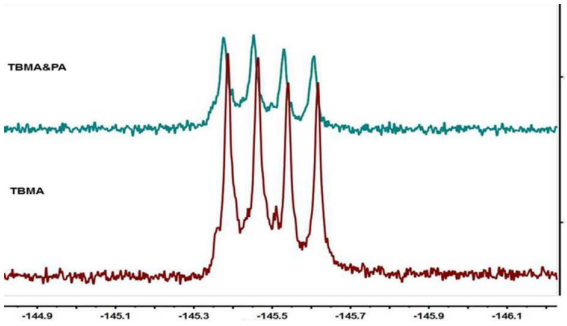

Fig. 10 ^{19}F NMR spectra of TBMA and the mixture of TBMA with PA in selected regions recorded in $CDCl_3$.

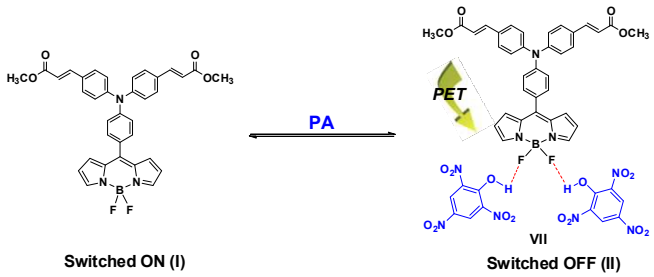

Scheme 2. Schematic Representation of the Fluorescence quenching.

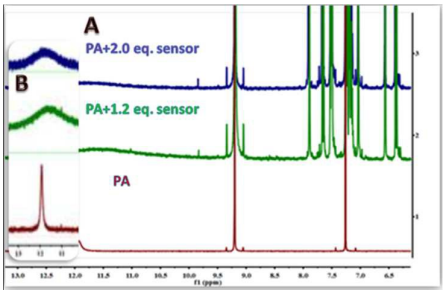

Fig. 11 ^{1}H NMR spectra of TBMA and PA with different mol ratio in $CDCl_3$.

Finding Detection Limit and Selective Detection of Nitroaromatics

We next investigated the fluorescence response of several other electron-deficient nitro compounds. Obviously, except PA, all other compounds shown insignificant quenching of the emission intensity, and the quenching efficiency are less than 30% (Fig. 12). According to the above results, BODIPY analogue of TBMA was proved as an effective and selective sensor for the detection of PA in solution. To determine the detection limit, fluorescence titration of TBMA in toluene with picric acid was carried out by adding picric acid solution and the fluorescence intensity as a function of picric acid added is then plotted. From this graph the concentration at which there is a sharp change in the fluorescence intensity multiplied with the concentration of

View Article Online
DOI: 10.1039/C5RA12154J

TBMA gave the detection limit.[58] Equation used for calculating detection limit (DL):DL= CL × CT, CL = Conc. of TBMA(1×10^{-6} M·L^{-1}); the datum of C_T (0.03 equiv) from Fig. S10. Thus, detection limit for picric acid DL = 1×10^{-6} M·L^{-1}× 0.03 equiv = 3×10^{-8} M·L^{-1} ~~= 30 ppb~~ . The quenching results could be quantitatively treated with the Stern-Volmer equation, $I_0/I= 1+ K_{sv}[PA]$,[26, 59-61] where I_0 and I stand for the fluorescence intensity of TBMA in the absence and presence of PA, respectively, [PA] is concentrations of PA, and K_{sv} is the Stern-Volmer constant. The decrease in the fluorescence intensity could be an electron transfer process on the basis of thermodynamic considerations as static and dynamic quenching. The Stern-Volmer plots shown two distinct regions: linear variation at a lower concentration of PA was mainly due to static quenching, whereas a steep curve at higher concentration of PA was presumably due to dynamic quenching. It can be seen that the Stern-Volmer plot of the change in the intensity of TBMA with respect to the PA concentration is linear at a lower concentration of PA and gives a quenching constant (K_{SV}) of 2.1×10^{-6} M^{-1}, suggesting the quenching of the fluorescence of TBMA ensemble upon the addition of PA is ascribed to the static quenching through a one-to-one nonfluorescent ground state complex, which after excitation returns to the ground state without emission of light (Fig. 13). Overall, the quenching constant and detection limit of the TBMA toward PA were noticeably higher than those reported in previous reports.[26]

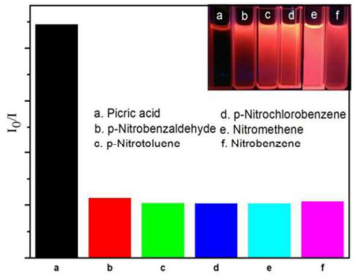

Fig. 12 Variation of fluorescence intensity (I_0/I) of TBMA toward different analytes in toluene.

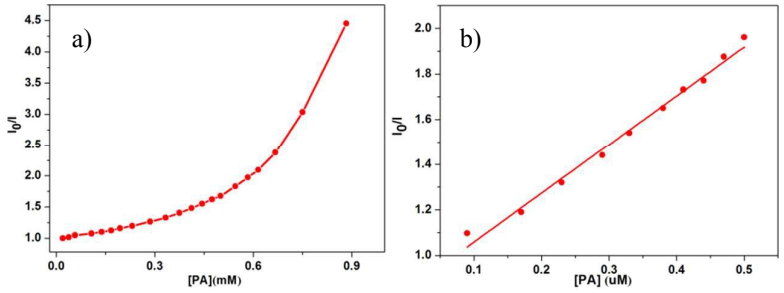

Fig. 13 (a) Stern−Volmer plots for TBMA(10 μM) using PA in toluene as quencher. (b) Stern−Volmer plots at lower concentration region of PA in toluene.

Experimental

Materials

Triphenylamine (TPA, 99%) is purchased from Energy Chemical Company. Pyrrole (>99%) is purchased from Energy Chemical Company. Trifluoroacetic acid (TFA, 99%) is purchased from Aladdin Reagent Company. phosphorus oxychloride ($POCl_3$) is purchased from Shandong Bazhou quartz clock Reagent Company. 2,3-Dichloro-5,6-dicyano-1,4-benzoquinone(DDQ, 98%) is purchased from Energy Chemical Company. Methyl acrylate (95%) is purchased from

View Article Online
DOI: 10.1039/C5RA12154J

Shuang-shuanghg Company. palladium acetate ($Pd(OAc)_2$, 99%), 1,3-bis(diphenylphosphino)propane (DPPP, 97%), tert-Butyl acrylate (99%), and methyl methacrylate (99%) are brought from Aladdin Reagent Company. Triethylamine (Et_3N, 99%) were purchased from Kaixinchem Company. Quinine sulfate dehydrate is purchased from Shanghai ZhongQin Company. Rhodamin B is purchased from Tianjin tianxin Fine chemical industry development center. Nitrogen with a purity of 99.99% is provided from commercial source. Other reagents, such as N,N-dimethylformamide (DMF), toluene, benzene, dichloromethane (DCM), methanol, ethanol, tetrahydrofuran (THF), ethyl acetate, diethyl ether, chloroform, 1,4-dioxane, tetrachloromethane, and acetic acid are A.R. grade.

Characterizations

^1H NMR (400 MHz), ^{13}C NMR (100 MHz), and H-H NOESY (400 MHz) spectra are recorded on a MERCURY spectrometer at 25 ^oC, and all NMR spectra are referenced to the solvent. Mass spectra are recorded on a HP5989B mass spectrometer. UV-visible absorption spectra are recorded on a TU-1901 spectrometer from 190 to 1100 nm. Fluorescence spectra are measured using a PE LS-55 Luminescence/Fluorescence Spectrophotometer. Emission spectra are recorded on a Perkin-Elmer LS 55 spectrofluorometer at room temperature (~25 °C) as well as other specific temperatures (0 to 65 °C). Fourier transform infrared (FT-IR) spectra are recorded on a DIGIL FTS3000 spectrophotometer using KBr tablets. The morphology of compounds is observed by scanning electron microscopy (SEM, ZEISS ULTRA PLUS). All the samples are prepared according to the standard methods. The ground-state geometries are fully optimized by using the density functional theory (DFT) at the B3LYP / 6-31G(d,p) level, as implemented in Gaussian 09.

Synthesis

Synthesis of I: Phosphorus oxychloride (15 mL) is added dropwise at 0 ^oC to DMF (15 mL), and the reaction mixture is stirred for 1 h. TPA(5g) is added and stirring is continued for 6 hours at 50 ^oC. The reaction mixture is poured in the 100 mL water slowly, whereby a yellow solid precipitated out. The solid is filtered, washed with water. Purification by column chromatography on silica gel (ethyl acetate/petroleumether,1:45) followed by recrystallization (CH_2Cl_2/hexane) gave II (4 g, 80%) as a yellow solid.[62,63] Mp 128-130 °C; ^1H NMR (400 MHz, $CDCl_3$) δ 9.81 (s, 1H), 7.68 (d, J = 8 Hz, 2H), 7.34 (t, J = 8 Hz, 4H), 7.16 – 7.19 (m, 6H), 7.02 (d, J = 8 Hz, 2H). ^{13}C NMR (100 MHz, CDCl3): δ 190.31, 153.31, 146.13, 131.24, 129.68, 129.12, 126.27, 125.06, 119.33 ppm. MS (FAB): m/z = 273.12 $[M+H]^+$. IR (KBr): 3098, 2827, 2740, 1689, 1585, 1504, 1488, 1427, 1330, 1259, 825, 757, 696 cm^{-1}.

Synthesis of II: In to a 100 mL, two-necked, round-bottom flask equipped with a condenser are placed 546 mg of I (2 mmol), 996 mg of potassium iodide (KI, 6 mmol), 1.284 g of potassium iodate (KIO_3, 6 mmol), and 10 mL of acetic acid. The mixture is heated to 70 ^oC under stirring for 10 h. The mixture is cooled to room temperature, filtration, washed consecutively with water and ammonia water to adjust the PH of the solution to be 8. the solution is extracted with CH_2Cl_2, The collected organic layer is washed with saturated sodium hydrogen sulfite and brine, dried over anhydrous Na_2SO_4.[64,65] After filtration and solvent evaporation, The crude product is recrystallized from ethanol to obtain the target II (461.1 mg, 85%) as a yellow solid. Mp 138-140 °C; ^1H NMR (400 MHz, $CDCl_3$) δ 9.84 (s, 1H), 7.71 (d, J = 8.0 Hz, 2H), 7.63 (d, J = 8.0 Hz, 4H), 7.05 (d, J = 8.0 Hz, 2H), 6.89 (d, J = 8.0 Hz, 4H) ppm. ^{13}C NMR (100 MHz, $CDCl_3$) δ

View Article Online
DOI: 10.1039/C5RA12154J

190.29, 152.17, 145.71, 138.85, 131.32, 130.35, 127.59, 120.76 ppm. MS(FAB): m/z=524.91 $[M+H]^+$. IR(KBr): 3441, 2805, 2733, 1689, 1598, 1574, 1327, 1315, 1270, 1217, 959, 819, 719 cm^{-1}.

Synthesis of III: 4-(bis(4-iodophenyl)amino)benzaldehyde（II）(2.63 g, 5 mmol), Methyl acrylate (12 mmol), $Pd(OAc)_2$ (18 mg, 0.08 mmol), 1,3-bis(diphenylphosphino)propane (DPPP, 66 mg, 0.16 mmol) and Et_3N (1.2 g, 12 mmol) are added into 10 mL of dry dimethylformamide (DMF). After stirring for 48 h at 80 °C under N_2 atmosphere. When the reaction is completed as determined by the disappearance of II, 20 mL of water is charged, and the solution is extracted with CH_2Cl_2 (3×10 mL). The organic phases are then dried with anhydrous magnesium sulfate, filtered, and concentrated under reduced pressure.[66] Purification by column chromatography on silica gel (ethyl acetate / petroleum ether, 1:10) followed by recrystallization (CH_2Cl_2/hexane) gave III (1.78 mg, 68%) as a yellow solid. Mp 133-135 °C; ^1H NMR (400 MHz, $CDCl_3$) δ 9.88 (s, 1H), 7.76 (d, J = 8.0 Hz, 2H), 7.66 (d, J = 16.0 Hz, 2H), 7.48 (d, J = 8.0Hz, 4H), 7.15 (t, J = 8.0Hz, 6H), 6.38 (d, J = 16.0 Hz, 2H), 3.81 (s, 6H) ppm. ^{13}C NMR (100 MHz, $CDCl_3$): δ 190.34, 167.35, 151.99, 147.70, 143.62, 131.30, 131.09, 130.85, 129.53, 125.37, 122.28, 117.24 ppm. MS (FAB): m/z = 441.1 6 $[M+H]^+$. IR(KBr): 3445, 2947, 2720, 1717, 1630, 1594, 1504, 1433, 1321, 1267, 1203, 1167, 1038, 980, 825 cm^{-1}.

Synthesis of TBMA: Pyrrole (5 mL, 72 mmol) and III (1.27 g, 2.88 mmol) are added to a dry 100 mL round-bottomed flask and degassed with a stream of N_2 for 5 min. TFA (22.2 μL, 0.5 mmol) was then added, and the solution is stirred under N_2 at room temperature. TLC analysis indicates that the disappearance of spots corresponds to III and appearance of a new spot corresponds to compound IV. The solvent is removed on a rotary evaporator under vacuum, and the crude compound is passed through flash silica gel column chromatography with a mixture of ethyl acetate and petroleum ether as eluent (1:6 by volume). The resultant compound IV (557 mg, 1 mmol) is dissolved in freshly distilled dichloromethane and oxidized with DDQ (272.4 mg, 1.2 mmol) for 30 min at room temperature. The reaction mixture is then treated with a small amount of Et_3N (5.6 mL, 40 mmol) followed by BF_3•OEt_2 (6.3 mL, 50 mmol), and the mixture is stirred for an additional 30 min at room temperature.[67] The solvent is removed in a rotary evaporator, and the resultant crude compound is purified by silica gel column chromatography with petroleum ether/ethyl acetate (3:1) and afforded pure TBMA (144.8mg, 26%) as a purple solid. Mp 205-207 °C; ^1H NMR (400 MHz, $CDCl_3$): δ 8.00 (s, 2H), 7.63 (d, J = 16.0 Hz, 2H), 7.41 (d, J = 8.2 Hz, 4H), 7.17 (d, J = 8.2 Hz, 2H), 7.06 (d, J = 6.7 Hz, 6H), 6.74 (s, 2H), 6.32 (d, J = 15.9 Hz, 2H), 6.18 (s, 2H), 5.94 (s, 2H), 5.46 (s, 1H), 3.80 (s, 6H) ppm. ^{13}C NMR (100 MHz, $CDCl_3$): δ 167.63 , 148.83 , 145.01 , 144.09 , 138.64 , 132.29 , 129.60 ,129.44 ,128.91 , 125.80 , 123.39 , 117.36 , 115.93 , 108.49 , 107.27 , 51.58 , 43.52 ppm. MS ESI m/z: 603.22 $[M+H]^+$. IR (KBr): 3419, 3232, 2944, 1710, 1630, 1591, 1507, 1453, 1412, 1387, 1324, 1263, 1182, 1117, 1076, 1046, 982, 911, 829, 777, 746, 715 cm^{-1}.

Synthesis of TB: Compound TB is synthesized in a manner similar to that for TBMA. Yield: 299.5 mg (77%); pure solid. Mp 212-214°C; ^1H NMR (400 MHz, $CDCl_3$) δ 7.90 (s, 2H), 7.40 (m, 6H), 7.23 – 7.06 (m, 10H), 6.55 (s, 2H) ppm. ^{13}C NMR (100 MHz, $CDCl_3$): δ 150.94, 147.52, 146.47, 142.77, 134.63, 132.25, 131.00, 129.67, 126.22, 125.94, 124.70, 120.02 , 117.95 ppm. MS (FAB): m/z = 435.17 $[M+H]^+$. IR (KBr) : 3105, 3059, 3036, 1587, 1558, 1533, 1488, 1412, 1388, 1332, 1294, 1261, 1224, 1192, 1118, 1076, 980, 911, 757, 742, 696 cm^{-1}.

View Article Online
DOI: 10.1039/C5RA12154J

Conclusions

In conclusion, TPA decorated BODIPY derivative of TBMA was designed and synthesized. Two tentacles like functional group of methyl acrylate modificated TPA core exerted huge steric hin-drance on the 8-position of BODIPY centre, therefore, TBMA exhibited emission wavelengths above 650 nm. Additionally, due to the soft interactions between the interlaced methyl acrylate groups, TBMA displayed notable AIE phenomenon in the mixture of THF and H_2O. We also discovered that TBMA could be applied as an efficient chemical sensor to PA detection. The detection limit and quenching constant (K_{SV}) are determined as 30 ppb and 2.1×10^{-6} M^{-1} respectively. ^{19}F NMR and ^{1}H NMR titration analysis verified that F···H hydrogen bonding is decserved as the interacting model, which is of possibility to facilitates the effective exciton migration.

Acknowledgements

The authors are grateful for the financial support of National Natural Science Foundation of China (No. 21202133, 21174114, 21361023). The authors also thank the Key Laboratory of Eco-Environment-Related Polymer Materials (Northwest Normal University), The Ministry of Education Scholars Innovation Team (IRT 1177) for financial support.

View Article Online
DOI: 10.1039/C5RA12154J

REFERENCES

[1] A. Treibs and F. -H. Kreuzer, *Liebigs Ann. Chem.,* 1968, **718**, 208-223.
[2] G. Ulrich, R. Ziessel and A. Harriman, *Angew. Chem., Int. Ed.*, 2008, **47**, 1184-1201.
[3] W. W. Qin and M. Baruah, *J. Phys. Chem. A*, 2005, **109**, 7371-7384.
[4] M. K. Kuimova, G. Yahioglu, J. A. Levitt and K. Suhling, *J. Am. Chem. Soc.*, 2008, **130**, 6672-6673.
[5] P. C. Eduardo, A. A. Angélica, G. D. Martha, L. Erik, Z. V. Rubi, G. V. Jazmin and V. G. Fabián, *Org. Lett.,* 2007, **9**, 3985-3988.
[6] M. Sameiro and T. Gonçalves, *Chem. Rev.*, 2009, **109**, 190-212;
[7] R. Hu, E. Lager and A. A. Angélica, *J. Phys. Chem. C*, 2009, **113**, 15845-15853.
[8] E. Fron, E. Coutiño-Gonzalez, L. Pandey, M. Sliwa, M. V. Auweraer, F. C. De Schryver, J. Thomas, Z. Dong, V. Leen, M. Smet, W. Dehaen and T. Vosch, *New J. Chem.*, 2009, **33**, 1490-1496.
[9] Y. Hong, J. W. Y. Lam and B. Z. Tang, *Chem. Soc. Rev.*, 2011, **40**, 5361-5388.
[10] J. Luo, J. W. Y. Lam, L. Cheng, H. Chen, C. Qiu, H. S. Kwok, X. Zhan, Y. Liu, D. Zhu and B. Z. Tang, *Chem. Commun.*, 2001, **18**, 1740-1741.
[11] J. Chen, C. C. W. Law, J. W. Y. Lam, Y. P. Dong, S. M. F. Lo, I. D. Williams, D. Zhu and B. Z. Tang, *Chem. Mater.* 2003, **15**, 1535-1546.
[12] Y. Hong, J. W. Y. Lam and B. Z. Tang, *Chem. Commun.* 2009, **29**, 4332-4353.
[13] J. Liu, J. W. Y. Lam and B. Z. Tang, *J. Inorg. Organomet. Polym. Mater.*, 2009, **19**, 249-285.
[14] L. Qian, J. Zhi, B. Tong, F. Yang, W. Zhao and Y. P. Dong, *Prog. Chem.,* 2008, **20**, 673-678.
[15] Y. Ma, H. Ma, Z. Yang, J. Ma, Y. Su, W. Li and Z. Lei, *Langmuir*, 2015, **31**, 4916-4923.
[16] H. Ma, Y. Ma, W. Li, F. Wang, F. Zhu, C. Qi, Z. Zhang, X. Yao and Z. Lei, *Macromol. Chem. Phys.,* 2014, **215**, 2305-2310.
[17] G. V. Perez and A. L. Perez, *J. Chem. Educ.*, 2000, **77**, 910-915.
[18] M. Nipper, Y. Qian, R. S. Carr and K. Mkiller, *Chemosphere,* 2004, **56**, 519-530.
[19] S. J. Toal and W. C. Trogler, *J. Mater. Chem.*, 2006, **16**, 2871-2883.
[20] H. Sohn, R. M. Calhoun, M. J. Sailor and W. C. Trogler, *Angew. Chem., Int. Ed.* 2001, **40**, 2104-2105.
[21] S. W. Thomas III, G. D. Joly and T. M. Swager, *Chem. Rev.* 2007, **107**, 1339-1386.
[22] K. K. Kartha, S. S. Babu, S. Srinivasan and A. Ajayghosh, *J. Am. Chem. Soc.*, 2012, **134**, 4834-4841.
[23] B. Roy, A. K. Bar, B. Gole, P. S. Mukherjee, *J. Org. Chem.*, 2013, **78**, 1306-1310.
[24] V. Sathish, A. Ramdass, Z. Z. Lu, M. Velayudham, P. Thanasekaran, K. L. Lu

View Article Online
DOI: 10.1039/C5RA12154J

and S. Rajagopal, *J. Phys. Chem. B*, 2013, **117**, 14358-14366.

[25] P. Thanasekaran, C. C. Lee and K. L. Lu, *Acc. Chem. Res.* 2012, **45**, 1403-1418.

[26] W. Li, H. Ma and Z. Lei, *RSC Adv.* 2014, **4**, 39351-39358.

[27] M. Benstead, G. H. Mehl and R. W. Boyle, *Tetrahedron*, 2011, **67**, 3573-3601.

[28] S. Hattori, K. Ohkubo, Y. Urano, H. Sunahara, T. Nagano, Y. Wada, N. V. Tkachenko, H. Lemmetyinen and S. Fukuzumi, *J. Phys. Chem. B*, 2005, **109**, 15368-15375.

[29] S. Erten-Ela, M. D. Yil¬maz, B. Icli, Y. Dede, S. Icli and E. U. Akkaya, *Org. Lett.*, 2008, **10**, 3299-3302.

[30] D. Kumaresan, R. P. Thummel, T. Bura, G. Ulrich and R. Ziessel, *Chem.-Eur. J.* , 2009, **15**, 6335-6339.

[31] C. Y. Lee and J. T. Hupp, *Langmuir*, 2010, **26**, 3760-3765.

[32] S. Kolemen, O. Bozdemir, A. Y. Cakmak, G. Barin, S. Erten-Ela, M. Marszalek, J. -H. Yum, S. M. Zakeeruddin, M. K. Nazeeruddin and M. Gratzel, *Chem. Sci.,* 2011, **2**, 949-954.

[33] J. Warnan, F. Buchet, Y. Pellegrin, E. Blart and F. Odobel, *Org. Lett.*, 2011, **13**, 3944-3947.

[34] O. A. Bozdemir, S. Erbas-Cakmak, O. O. Ekiz, A. Dana and E. U. Akkaya, *Angew. Chem., Int. Ed.*, 2011, **50**, 10907-10912.

[35] N. Boens, V. Leen and W. Dehaen, *Chem. Soc. Rev.*, 2012, **41**,1130-1172.

[36] N. Boens, W. Qin, M. Baruah, W. M. DeBorggraeve, A. Filarowski, N. Smisdom, M. Ameloot, L. Crovetto, E. M. Talavera and J. M. Alvarez-Pez, *Chem.-Eur. J.*, 2011, **17**, 10924-10934.

[37] M. J. Ortiz, I. García-Moreno, A. R. Agarrabeitia, G. Dura-Sampedro, A. Costela, R. Sastre, F. LopezArbeloa, J. BanuelosPrieto and I. LopezArbeloa, *Phys. Chem. Chem. Phys.*, 2010, **12**, 7804-7811.

[38] M. Benstead, G. H. Mehl and R. W. Boyle, *Tetrahedron*, 2011, **67**, 3573-3601.

[39] R. Ziessel, G. Ulrich and A. Harriman, *New J. Chem.,* 2007, **31**, 496-501.

[40] R. W. Wagner and J. S. Lindsey, *Pure & Appl. Chem.*, 1996, **68**, 1373-1380.

[41] S. Madhu, M. R. Rao and M. S. Shaikh, *Inorg. Chem.*, 2011, **50**, 4392-4400.

[42] Z. R. Grabowski, K. Rotkiewics and W. Rettig, *Chem. Rev.*, 2003, **103**, 3899-4032.

[43] E. Lippert, W. Rettig, V. Bonacic-Koutecky, F. Hei-sel and J. A. Miehe, *Adv. Chem. Phys.*, John Wiley & Sons, New York, 1987, vol. **68**, pp. 1-174.

[44] J. S. Yang, K. L. Liau, C. Y. Li and M. Y. Chen, *J. Am. Chem. Soc.*, 2007, **129**, 13183-13192.

[45] S. Cogan, S. Zilberg and Y. Haas, *J. Am. Chem. Soc.*, 2006, **128**, 3335-3345.

[46] J. N. Demas and G. A. Grosby, *J. Phys. Chem.*, 1971, 75, 991-1024.

[47] W. R. Ware and W. Rothman, *Chem. Phys. Lett.*, 1976, 39, 449-453.

[48] C. A. Parker and W. T. Rees, *Analyst,* 1960, 85, 587-600.

[49] E. Lager, J. Liu and A. A. Angélica, *J. Org. Chem.*, 2009, **74**, 2053-2058.

[50] Y. N. Hong, J. W. Y. Lam and B. Z. Tang, *Chem. Soc. Rev.*, 2011, **40**, 5361-5388.

View Article Online
DOI: 10.1039/C5RA12154J

[51] W. Z. Yuan, Y. Q. Tan, Y. Y. Gong, P. Lu, J. W. Y. Lam, X. Y. Shen, C. F. Feng, H. H. Y. Sung, Y. W. Lu, I. D. Williams, J. Z. Sun, Y. M. Zhang and B. Z. Tang, *Adv. Mater.*, 2013, **25**, 2837-2843.

[52] Z. K. Wang, S. J. Chen, J. W. Y. Lam, W. Qin, R. T. K. Kwok, N. Xie, Q. L. Hu and B. Z. Tang, *J. Am. Chem. Soc.*, 2013, **135**, 8238-8245.

[53] M. Vybornyi, A. V. Rudnev, S. M. Langenegger, T. Wandlowski, G. Calzaferri and R. Haner, *Angew. Chem., Int. Ed.*, 2013, **52**, 11488-11493.

[54] Y. Liu, S. Chen, J. W. Y. Lam, P. Lu, R. T. K. Kwok, F. Mahtab, H. S. Kwok and B. Z. Tang, *Chem. Mater.*, 2011, **23**, 2536-2544.

[55] Z. Zhao, C. Deng, S. Chen, J. W. Y. Lam, W. Qin, P. Lu, Z. Wang, H. S. Kwok, Y. Ma, H. Qiu and B. Z. Tang, *Chem. Commun.*, 2011, **47**, 8847-8849.

[56] A. C. Benniston, G. Copley, K. J. Elliott, R. W. Harrington and W. Clegg, *Eur. J. Org. Chem.*, 2008, **16**, 2705-2713.

[57] V. Lakshmi and M. Ravikanth, *J. Org. Chem.,* 2011, **76**, 8466-8471.

[58] D. A. Olley, E. J. Wren, G. Vamvounis, M. J. Fernee, X. Wang, P. L. Burn, P. Meredith and P. E. Shaw, *Chem. Mater.*, 2011, **23**, 789-794.

[59] E. Ballesteros, D. Moreno, T. Gomez, T. Rodriguez, J. Rojo, M. G. Valverde and T. Torroba, *Org. Lett.*, 2009, **11**, 1269-1272.

[60] P. Lasitha and Edamana Prasad, *RSC Adv.*, 2015, **5**, 41420-41427.

[61] J. Xiong, J. Li, G. Mo, J. Huo, J. Liu, X. Chen, and Z. Wang, *J. Org. Chem.,* 2014, **79**, 11619-11630

[62] T. Mallegol, S. Gmouh, M. A. A. Meziane, M. Blanchard-Desce, *O.* Mongin, *Synthesis,* 2005, **11**, 1771-1774.

[63] Y. Wang and M. Leung, *Macromolecules*, 2011, **44**, 8771-8779.

[64] L. Porrès, O. Mongin, C. Katan and M. Charlot, *Org. Lett.* 2004, **6**, 47-50.

[65] W. Z. Yuan, Y. Gong, S. Chen, X. Y. Shen, J. W. Y. Lam, P. Lu, Y. Lu, Z. Wang, R. Hu, N. Xie and B. Z. Tang, *Chem. Mater.* 2012, **24**, 1518-1528.

[66] T. J. Kwok and J. A. Virgilio, *Org. Process Res. Dev.*, 2005, **9**, 694-696.

[67] P. Thamyongkit, A. D. Bhise, M. Taniguchi and J. S. Lindsey, *J. Org. Chem.*, 2006, **71**, 903-910.